Sphere Covering for Poisson Processes

Hui-An Shen
University of Bern and
University of Zurich, Switzerland
huian.shen@unibe.ch

Stefan M. Moser
ETH Zürich, Switzerland and
NCTU, Taiwan
moser@isi.ee.ethz.ch

Jean-Pascal Pfister
University of Bern and
University of Zurich, Switzerland
jeanpascal.pfister@unibe.ch

Abstract—The geometric interpretation of sphere covering describing the rate distortion problem of a Gaussian source with the squared-error distortion measure is generalized to a Laplacian source and the ℓ_1-distortion measure. Using additional constraints on the distortion measure, sphere covering is further generalized to exponential sources and to Poisson point processes.

I. INTRODUCTION

It is well-known that the rate-distortion problem of a Gaussian source and a squared-error distortion measure can be understood geometrically by counting the minimum number of small distortion balls required to completely cover the volume of the ball describing the possible outputs of the Gaussian source [1, Sec. 10.9], [2, Sec. 10.5]. This beautiful picture of *sphere covering*,[1] however, is not restricted to the special case of Gaussian sources with an ℓ_2-distortion measure, but can be generalized to sources and corresponding distortion measures in the general ℓ_p-space. In this paper, we focus on the case for $p = 1$, i.e., a Laplacian source with the ℓ_1-distortion measure, and then show how it can be adapted to find a corresponding geometric interpretation of the well-known rate-distortion function of a Poisson point process. The general case in ℓ_p is deferred to a later publication.

The remainder of this paper is structured as follows. After some definitions and comments about notation in Section II, we briefly recall the well-known sphere covering interpretation for the Gaussian source in Section III. In Section IV we then develop sphere covering in ℓ_1 for a Laplacian source. Section V adapts the results from Section IV to allow the description of an exponential source (and a constrained distortion measure), and Section VI finally looks at the Poisson point processes. We focus on geometric proofs for the converse part of the rate-distortion problem and omit the achievability proofs.

II. NOTATION

The ℓ_p^n-*ball* in $\mathbb{R}^n$ around the center $\hat{\mathbf{x}} \in \mathbb{R}^n$ of radius $r > 0$ is given as

$$\mathcal{B}_p^n(r, \hat{\mathbf{x}}) \triangleq \left\{ \mathbf{x} \in \mathbb{R}^n : \left(\sum_{i=1}^n |x_i - \hat{x}_i|^p \right)^{1/p} \leq r \right\}, \quad (1)$$

[1]A similar geometric interpretation exists for the channel coding problem leading to *sphere packing* [3, Sec. 17.3], [2, Ch. 9].

and its surface, the ℓ_p^n-*sphere* in $\mathbb{R}^n$, is

$$\mathcal{S}_p^{n-1}(r, \hat{\mathbf{x}}) \triangleq \left\{ \mathbf{x} \in \mathbb{R}^n : \left(\sum_{i=1}^n |x_i - \hat{x}_i|^p \right)^{1/p} = r \right\}. \quad (2)$$

For the n-simplex in $\mathbb{R}^n$ around the center $\hat{\mathbf{x}} \in \mathbb{R}^n$ we write

$$\triangle^{n-1}(r, \hat{\mathbf{x}}) \triangleq \left\{ \mathbf{x} \in \mathbb{R}^n : \sum_{i=1}^n (x_i - \hat{x}_i) = r, \right.$$
$$\left. x_i - \hat{x}_i > 0, \ \forall i \in \{1, \ldots, n\} \right\}. \quad (3)$$

Sometimes we omit the second argument in the sets given in (1)–(3), in which case it is understood that a vector $\mathbf{0}$ should be substituted, i.e., $\mathcal{B}_p^n(r) \triangleq \mathcal{B}_p^n(r, \mathbf{0})$, $\mathcal{S}_p^{n-1}(r) \triangleq \mathcal{S}_p^{n-1}(r, \mathbf{0})$, and $\triangle^{n-1}(r) \triangleq \triangle^{n-1}(r, \mathbf{0})$.

We use vol_n to denote the n-dimensional Lebesgue measure. Bold font denotes vectors (e.g., $\mathbf{x}$ and $\mathbf{0}$), and sets are in a calligraphic font $\mathcal{B}$. The logarithm $\log(\cdot)$ is to base 2.

III. RATE DISTORTION AND SPHERE COVERING IN ℓ_2

We recall the familiar geometric picture for the Gaussian-quadratic rate-distortion problem based on sphere covering. For a Gaussian source of variance σ^2 and mean 0, the rate-distortion code with distortion D yields a minimal rate given by taking the volume ratio of the *source ball* $\mathcal{B}_2^n(\sqrt{n\sigma^2})$ and the *distortion ball* $\mathcal{B}_2^n(\sqrt{nD})$ in $\mathbb{R}^n$, i.e.,

$$R_{\text{Gaussian}}(D) = \lim_{n \to \infty} \frac{1}{n} \log \frac{\text{vol}_n\left(\mathcal{B}_2^n(\sqrt{n\sigma^2}) \right)}{\text{vol}_n\left(\mathcal{B}_2^n(\sqrt{nD}) \right)}. \quad (4)$$

Note that the length-n codewords that achieve (4) are the coordinates of the centers of the distortion balls. While we know that optimal codewords can be generated IID according to a Gaussian distribution of variance $\sigma^2 - D$ and mean 0, this fact cannot be deduced from the sphere-covering argument easily if we follow the geometric picture as given in Fig. 1(a), where the n-dimensional distortion balls cover the n-dimensional source ball.

To infer the generation of rate-distortion codewords, we need an alternative geometric picture, as already explored in [4, Sec. I], which we depict in Fig. 1(b): Here we note that the source sequences generated by the Gaussian source actually lie within a thin layer close to the *surface* of the

source ball almost surely. Therefore, we aim to *enclose*[2] the *surface* of the source ball entirely with a minimal number of distortion balls, i.e., cover the surface $\mathcal{S}_2^{n-1}(\sqrt{n\sigma^2})$ with the cross sections $\mathcal{S}_2^{n-1}(\sqrt{n\sigma^2}) \cap \mathcal{B}_2^n(\sqrt{nD}, \hat{\mathbf{x}}_m)$, where the codewords $\hat{\mathbf{x}}_m$ are selected such that each cross section is maximized. From Fig. 1(b), one immediately sees that all $\hat{\mathbf{x}}_m$ lie on the surface of an ℓ_2^n-ball:

$$\hat{\mathbf{x}}_m \in \underset{\hat{\mathbf{x}} \in \mathbb{R}^n}{\arg\max} \, \mathrm{vol}_{n-1}\left(\mathcal{S}_2^{n-1}(\sqrt{n\sigma^2}) \cap \mathcal{B}_2^n(\sqrt{nD}, \hat{\mathbf{x}})\right) \quad (5)$$

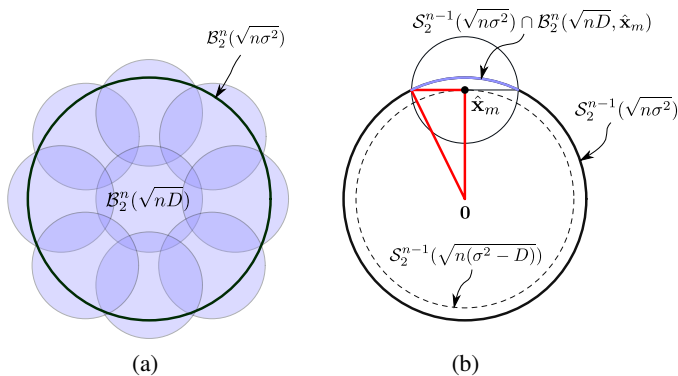$$= \mathcal{S}_2^{n-1}\left(\sqrt{n(\sigma^2 - D)}\right). \quad (6)$$

Figure 1. Geometric picture of ℓ_2 sphere covering: on the left all distortion balls cover the source ball, while on the right only the surface of the source ball is covered.

To this point, one may conjecture that the relationship between rate distortion and sphere covering exists beyond the well-known case for the Gaussian source in the ℓ_2-space presented in this section. In the following sections we present our results for an analogous case of sphere covering with ℓ_1^n-balls in $\mathbb{R}^n$, define its corresponding rate-distortion problem, extend it to an exponential source, and finally link it to known rate-distortion functions for the Poisson process.

IV. RATE DISTORTION AND SPHERE COVERING IN ℓ_1

A. The Laplacian-ℓ_1 Rate-Distortion Problem

To generalize the ideas of Section III to the ℓ_1-space we consider the Laplacian source

$$X \sim P_X(x) \triangleq \frac{1}{2r_0} e^{-|x|/r_0} \quad (7)$$

and choose the ℓ_1-distortion measure

$$d(x, \hat{x}) \triangleq |x - \hat{x}|. \quad (8)$$

Then, by recalling the standard definition

$$d(\mathbf{x}, \hat{\mathbf{x}}) \triangleq \frac{1}{n} \sum_{i=1}^n d(x_i, \hat{x}_i) = \frac{1}{n} \sum_{i=1}^n |x_i - \hat{x}_i|, \quad (9)$$

---

[2]The phrase "enclose a surface" is used when we refer to covering an arbitrarily small *inflation* of this $(n-1)$-dimensional surface in $\mathbb{R}^n$ for n sufficiently large.

one immediately realizes that the distortion ball[3] centered at $\hat{\mathbf{x}}$ is by definition an ℓ_1^n-ball, i.e.,

$$\{\mathbf{x} \in \mathbb{R}^n : d(\mathbf{x}, \hat{\mathbf{x}}) \le D\} = \mathcal{B}_1^n(nD, \hat{\mathbf{x}}). \quad (10)$$

In a naive approach we can now argue that, for large n, the source sequence $\mathbf{X}$ will lie with high probability within the ℓ_1^n-ball of radius nr_0, $\mathcal{B}_1^n(nr_0)$. Thus, by computing the ratio of the volume of the large radius-(nr_0) ball to the volume of the small radius-(nD) balls, we can easily deduce the minimum number of codewords needed to cover the complete source ball:

$$|\mathcal{C}^n| \ge \frac{\mathrm{vol}_n\big(\mathcal{B}_1^n(nr_0)\big)}{\mathrm{vol}_n\big(\mathcal{B}_1^n(nD)\big)} = \left(\frac{r_0}{D}\right)^n \quad (11)$$

(see Fig. 2(a)). From this, the rate-distortion function (or rather a lower bound to it) can be derived using that the rate is defined as
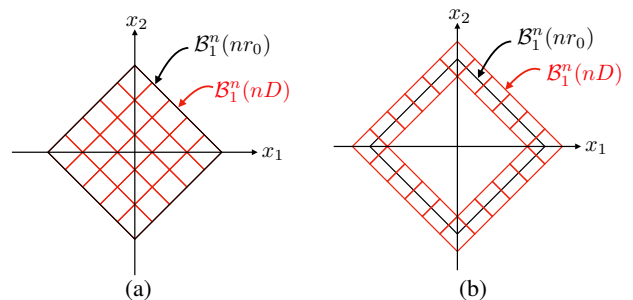
$$R = \frac{1}{n} \log |\mathcal{C}^n|. \quad (12)$$

Figure 2. Geometric picture of ℓ_1 sphere covering, analogous to the ℓ_2 sphere covering shown in Fig. 1.

We would like to present a more accurate geometric picture by observing that the source sequences generated by P_X lie within a thin layer at the *surface* of the source ball $\mathcal{B}_1^n(nr_0)$ almost surely, since $\frac{1}{n} \sum_{i=1}^n |x_i| \to r_0$ with probability 1 as $n \to \infty$ [5, Sec. II].

Thus, reminiscent of Section III, we aim to *enclose* the surface of the source ball with a minimal number of distortion balls, i.e., we intersect the source ℓ_1-sphere with many small distortion balls, creating tiles that cover the complete surface of the source ball, see Fig. 2(b).

Theorem 1: For a Laplacian source (7) and an ℓ_1-distortion measure (8), define $D \triangleq \lim_{n \to \infty} \mathsf{E}\big[d(\mathbf{X}, \hat{\mathbf{X}})\big]$. Then the rate-distortion function is lower-bounded as

$$R_{\mathrm{Laplacian}}(D) \ge \begin{cases} \log\left(\frac{r_0}{D}\right) & \text{if } 0 < D \le r_0, \\ 0 & \text{otherwise.} \end{cases} \quad (13)$$

Proof: This theorem follows from Theorem 3 below. ∎

---

[3]Note that we follow common practice and talk about ℓ_1^n-*balls* and ℓ_1^n-*spheres*, even though the corresponding shape does not look like a traditional ball at all, but rather is a higher-dimensional version of the three-dimensional regular octahedron. See also Fig. 2.

B. Sphere Covering with ℓ_1^n-Balls in $\mathbb{R}^n$

When investigating ways of how a small ℓ_1^n-ball can cover a large ℓ_1^n-sphere (see Fig. 2(b)), we will avoid distinguishing various different cases of covering facets, edges, or corners, but rather directly prove that the covered ($(n-1)$-dimensional) part of the large ℓ_1^n-sphere is upper-bounded by the surface of the small ℓ_1^n-ball.

Proposition 2: For radii $r_\mathrm{b} > r_\mathrm{s}$, and arbitrary $\mathbf{z}$,

$$\mathrm{vol}_{n-1}\big(\mathcal{S}_1^{n-1}(r_\mathrm{b}) \cap \mathcal{B}_1^n(r_\mathrm{s}, \mathbf{z})\big) \leq \mathrm{vol}_{n-1}\big(\mathcal{S}_1^{n-1}(r_\mathrm{s}, \mathbf{z})\big). \quad (14)$$

Proof: See Appendix A. ∎

Theorem 3 (Asymptotic sphere covering in ℓ_1^n): For $n \geq 2$, fix two radii $r_\mathrm{b} > r_\mathrm{s} > 0$ and denote by $\mathcal{C}^n \triangleq \{\hat{\mathbf{x}}_i \in \mathbb{R}^n\}$ a collection of centers of ℓ_1^n-balls $\mathcal{B}_1^n(r_\mathrm{s}, \hat{\mathbf{x}}_i)$. Then for any $\mathcal{C}^n$ such that the union of radius-r_s balls around the centers in $\mathcal{C}^n$ do cover the complete surface of the radius-r_b ball,

$$\mathcal{S}_1^{n-1}(r_\mathrm{b}) \subseteq \bigcup_{\hat{\mathbf{x}} \in \mathcal{C}^n} \mathcal{B}_1^n(r_\mathrm{s}, \hat{\mathbf{x}}), \quad (15)$$

the following inequality holds:

$$\lim_{n \to \infty} \frac{1}{n} \log |\mathcal{C}^n| \geq \log\left(\frac{r_\mathrm{b}}{r_\mathrm{s}}\right). \quad (16)$$

Proof: The minimal size of $\mathcal{C}^n$ is achieved when $\hat{\mathbf{x}}_i$ are selected such that $\mathrm{vol}_{n-1}\big(\mathcal{S}_1^{n-1}(r_\mathrm{b}) \cap \mathcal{B}_1^n(r_\mathrm{s}, \hat{\mathbf{x}})\big)$ is maximized. From Proposition 2 we know that the latter is upper-bounded by the boundary measure of the small ball. Thus,

$$|\mathcal{C}^n| \geq \frac{\mathrm{vol}_{n-1}\big(\mathcal{S}_1^{n-1}(r_\mathrm{b})\big)}{\max_{\hat{\mathbf{x}}} \mathrm{vol}_{n-1}\big(\mathcal{S}_1^{n-1}(r_\mathrm{b}) \cap \mathcal{B}_1^n(r_\mathrm{s}, \hat{\mathbf{x}})\big)} \quad (17)$$

$$\geq \frac{\mathrm{vol}_{n-1}\big(\mathcal{S}_1^{n-1}(r_\mathrm{b})\big)}{\mathrm{vol}_{n-1}\big(\mathcal{S}_1^{n-1}(r_\mathrm{s})\big)} = \left(\frac{r_\mathrm{b}}{r_\mathrm{s}}\right)^{n-1} \quad (18)$$

and hence (16) holds. ∎

V. RATE DISTORTION AND SPHERE COVERING IN ℓ_1 WITH CONSTRAINED ℓ_1-DISTORTION MEASURE

In Section IV, we have shown that the Laplacian-ℓ_1 rate-distortion problem turns out to have the geometric picture of sphere covering in ℓ_1, in complete analogy to the association of the Gaussian-quadratic case to sphere covering in the ℓ_2-space. In this section, we will show that by adding an additional constraint on the ℓ_1-distortion measure to break the symmetry, we can also use our geometric picture of sphere covering to explain rate distortion of an exponential source. The ultimate goal of this description will be the corresponding rate-distortion problem of a Poisson process, which can be described by the exponentially distributed inter-arrival times; see Section VI.

To motivate our choice of the constrained ℓ_1-distortion measure, we make the following preliminary observations:

1) The interval description for point process realizations with a fixed number of points over duration T forms a simplex (because the sum of all intervals must equal T), and

2) with reflections, this simplex becomes the surface (boundary) of an ℓ_1^n-ball.

In view of these two observations, we use as a distortion measure the common ℓ_1-distortion, but with the additional twist that the distortion is set to infinity if the sequences do not satisfy some specified condition. The effect of this additional constraint is to break the symmetry that was introduced in order to arrive at an ℓ_1^n-ball from the implicitly given simplex.

A. The Exponential-ℓ_1 Rate-Distortion Problem

Consider the exponential source

$$X \sim P_X(x) = \lambda\, e^{-\lambda x}\, \Theta(x), \quad (19)$$

where $\Theta(\cdot)$ denotes the Heaviside function, and define the following constrained ℓ_1-distortion measure.

Definition 4 (Constrained ℓ_1-distortion measure):

$$d_1(\mathbf{x}, \hat{\mathbf{x}}) \triangleq \begin{cases} \dfrac{1}{n} \displaystyle\sum_{i=1}^n |x_i - \hat{x}_i| & \text{if } x_i - \hat{x}_i \geq 0 \text{ for } i \text{ odd} \\ & \text{and } x_i - \hat{x}_i < 0 \text{ for } i \text{ even,} \\ \infty & \text{otherwise.} \end{cases} \quad (20)$$

Remark 5: Choosing alternating signs as the condition under which the constrained ℓ_1-distortion $d_1(\cdot, \cdot)$ is finite rather than, e.g., requiring the first half to be positive and the second half negative, makes the condition applicable still as $n \to \infty$.

Remark 6: The *one-sided distortion measure* for an exponential source proposed by Verdú [6], [7] is similar to Definition 4, only that the constraint is imposed such that $x_i - \hat{x}_i \geq 0$ for all $i \in \{1, 2, \ldots, n\}$.

Theorem 7: For an exponential source (19) and the constrained ℓ_1-distortion measure (20), define $D \triangleq \lim_{n \to \infty} \mathsf{E}\big[d_1(\mathbf{X}, \hat{\mathbf{X}})\big]$. Then the rate-distortion function is lower-bounded as

$$R_{\text{Exponential}}(D) \geq \begin{cases} -\log(\lambda D) & \text{if } 0 < D \leq \frac{1}{\lambda}, \\ 0 & \text{otherwise.} \end{cases} \quad (21)$$

Proof: This theorem follows from Theorem 11 below. ∎

B. Sphere Covering with Constrained ℓ_1^n-Balls in $\mathbb{R}^n$

The exponential source specified by (19) can be viewed as the Laplacian source in (7) renormalized over the positive support $x \geq 0$. As opposed to lying almost surely on the surface of an ℓ_1^n-ball for the Laplacian source (as n tends to infinity), the sequences generated by the exponential source (19) lie instead almost surely on a simplex $\triangle^{n-1}(n/\lambda)$ in $\mathbb{R}^n$ as n tends to infinity.

Since we use the constrained ℓ_1-distortion measure given in (20), in the corresponding geometry of the problem, the distortion ball is also constrained: it is an orthant of the ℓ_1^n-ball $\mathcal{B}_1^n(r_\mathrm{s})$, i.e., it becomes a (nonregular) n-simplex, called *distortion simplex*.

Definition 8: For $\hat{\mathbf{x}} \in \mathbb{R}^n$ and $r_\mathrm{s} > 0$, we define the *distortion simplex* $\mathcal{U}_1^n(r_\mathrm{s}, \hat{\mathbf{x}})$ as the intersection of $\mathcal{B}_1^n(r_\mathrm{s}, \hat{\mathbf{x}})$ with n half-spaces as follows:

$$\mathcal{U}_1^n(r_\mathrm{s}, \hat{\mathbf{x}}) \triangleq \Big\{ \mathbf{x} \in \mathbb{R}^n : \mathbf{x} \in \mathcal{B}_1^n(r_\mathrm{s}, \hat{\mathbf{x}}), \text{ and } x_i - \hat{x}_i \geq 0 \text{ for}$$
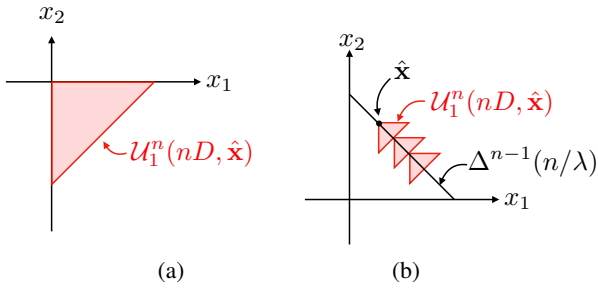
Figure 3. Geometric picture of sphere covering of the simplex $\triangle^{n-1}(n/\lambda)$ of the exponential source (b) with many small distortion simplices (a).

$$i \text{ odd}, x_i - \hat{x}_i < 0 \text{ for } i \text{ even}\Big\}. \tag{22}$$

As before, we use the shorthand notation $\mathcal{U}_1^n(r_s) \triangleq \mathcal{U}_1^n(r_s, \mathbf{0})$.

Thus, we need to cover the simplex $\triangle^{n-1}(n/\lambda)$ of the exponential source (which is the first orthant of the original large ℓ_1^n-sphere) with many small distortion simplices, see Fig. 3(b).

We use $\mathcal{H}$ to denote any hyperplane of $\mathbb{R}^n$ that is parallel to $\mathcal{H}_0$, where $\mathcal{H}_0$ is the hyperplane $x_1 + \cdots + x_n = 0$.

Proposition 9 (The maximal hyperplane section of $\mathcal{U}_1^n(1)$ is the facet $\triangle^{n-1}(1)$): Let $\mathcal{K}$ be any hyperplane in $\mathbb{R}^n$. Then

$$\text{vol}_{n-1}\big(\triangle^{n-1}(1)\big) = \max_{\mathcal{K}} \text{vol}_{n-1}\big(\mathcal{K} \cap \mathcal{U}_1^n(1)\big). \tag{23}$$

Proof: See Appendix B. ∎

Corollary 10: Note that since Proposition 9 makes no assumptions about the hyperplane, it follows directly that also sections with a parallel hyperplane $\mathcal{H}$ cannot be larger than the facet $\triangle^{n-1}(1)$, i.e., $\forall n \geq 2$,

$$\max_{\mathcal{H}} \text{vol}_{n-1}\big(\mathcal{H} \cap \mathcal{U}_1^n(1)\big) \leq \text{vol}_{n-1}\big(\triangle^{n-1}(1)\big). \tag{24}$$

The following theorem is parallel to Theorem 3.

Theorem 11 (Asymptotic ℓ_1-covering of a simplex): For $n \geq 2$, fix two radii $r_b > r_s > 0$ and denote by $\mathcal{C}^n \triangleq \{\hat{\mathbf{x}}_i \in \mathbb{R}^n\}$ a collection of centers of distortion simplices $\mathcal{U}_1^n(r_s, \hat{\mathbf{x}}_i)$. Then for any $\mathcal{C}^n$ such that

$$\triangle^{n-1}(r_b) \subseteq \bigcup_{\hat{\mathbf{x}} \in \mathcal{C}^n} \mathcal{U}_1^n(r_s, \hat{\mathbf{x}}), \tag{25}$$

the following inequality holds:

$$\lim_{n \to \infty} \frac{1}{n} \log |\mathcal{C}^n| \geq \log\left(\frac{r_b}{r_s}\right). \tag{26}$$

Proof: The minimal size of $\mathcal{C}^n$ is achieved when $\hat{\mathbf{x}}_i$ are selected such that $\text{vol}_{n-1}\big(\triangle^{n-1}(r_b) \cap \mathcal{U}_1^n(r_s, \hat{\mathbf{x}})\big)$ is maximized:

$$|\mathcal{C}^n| \geq \frac{\text{vol}_{n-1}\big(\triangle^{n-1}(r_b)\big)}{\max_{\hat{\mathbf{x}}} \text{vol}_{n-1}\big(\triangle^{n-1}(r_b) \cap \mathcal{U}_1^n(r_s, \hat{\mathbf{x}})\big)} \tag{27}$$

$$\geq \frac{\text{vol}_{n-1}\big(\triangle^{n-1}(r_b)\big)}{\max_{\mathcal{H}} \text{vol}_{n-1}\big(\mathcal{H} \cap \mathcal{U}_1^n(r_s, \mathbf{0})\big)} \tag{28}$$

$$\geq \frac{\text{vol}_{n-1}\big(\triangle^{n-1}(r_b)\big)}{\text{vol}_{n-1}\big(\triangle^{n-1}(r_s)\big)} = \left(\frac{r_b}{r_s}\right)^{n-1}. \tag{29}$$

Here, in (28) we replace the large simplex by a hyperplane; and the inequality in (29) uses (24) in Corollary 10. ∎

VI. RATE DISTORTION AND SPHERE COVERING FOR THE HOMOGENEOUS POISSON PROCESS

In this section, we will show that the rate-distortion problem for a homogeneous Poisson process has a geometric picture that basically coincides with the constrained ℓ_1-sphere covering discussed in Section V. The main idea is to describe the Poisson point process using the exponentially distributed inter-point intervals and then rely on the results from Section V.

Define a function f that takes as an input a point process realization $\mathbf{y}$ over the interval $[0, T]$ and returns a vector containing the inter-point intervals of $\mathbf{y}$, i.e.,

$$f(\mathbf{y}) = \boldsymbol{\tau} \triangleq (\tau_0, \tau_1, \ldots, \tau_m), \tag{30}$$

where for all $k \in \{1, 2, \ldots, m\}$, the kth point is at $y_k = \sum_{i=0}^{k-1} \tau_i$ and where $\sum_{i=0}^{m} \tau_i = T$.

Let $\mathbf{Y}$ be a Poisson point process $\mathbf{Y}$ over the interval $[0, T]$ and let $\mathbf{y}$ be a realization of $\mathbf{Y}$. Thus, the number of components of $f(\mathbf{Y})$ is distributed as follows:

$$\Pr\big[|f(\mathbf{Y})| = m\big] = \frac{e^{-\lambda T}(\lambda T)^{m-1}}{(m-1)!}, \quad m \in \mathbb{N}. \tag{31}$$

Here we use the shorthand $|\mathbf{z}|$ to denote the number of components of a vector $\mathbf{z}$.

To study the rate-distortion problem for a Poisson process, we need to define a distortion measure for any two point processes $\mathbf{Y}$ and $\hat{\mathbf{Y}}$ in continuous time over the interval $[0, T]$, denoted $d_T(\mathbf{y}, \hat{\mathbf{y}})$ for point process realizations $\mathbf{y}$ and $\hat{\mathbf{y}}$. Using the constrained ℓ_1-distortion measure $d_1(\cdot, \cdot)$ in (20), we choose

$$d_T(\mathbf{y}, \hat{\mathbf{y}}) \triangleq \begin{cases} \frac{|f(\mathbf{y})|}{T} d_1\big(f(\mathbf{y}), f(\hat{\mathbf{y}})\big) & \text{if } |f(\mathbf{y})| = |f(\hat{\mathbf{y}})|, \\ \infty & \text{otherwise.} \end{cases} \tag{32}$$

Define

$$\bar{D} \triangleq \lim_{T \to \infty} \mathsf{E}\big[d_T(\mathbf{Y}, \hat{\mathbf{Y}})\big]. \tag{33}$$

Theorem 12 (Poisson-ℓ_1 rate-distortion problem): The rate-distortion function (in *bits per unit time*) of a Poisson point process $\mathbf{Y}$ with intensity λ under the distortion measure (32) is lower-bounded as

$$R_{\text{Poisson}}(\bar{D}) \geq \begin{cases} -\lambda \log \bar{D} & \text{if } 0 < \bar{D} \leq 1, \\ 0 & \text{otherwise.} \end{cases} \tag{34}$$

Proof: The proof of Theorem 12 relies[4] on Theorem 7. Let $\mathbf{y}$ be a realization of the Poisson point process $\mathbf{Y}$ over the interval $[0, T]$. Note that as T tends to infinity, $|f(\mathbf{Y})|$ tends to λT almost surely. Thus, for $|f(\mathbf{Y})| = |f(\hat{\mathbf{Y}})|$, we can write (32) asymptotically as

$$\lim_{T \to \infty} d_T(\mathbf{Y}, \hat{\mathbf{Y}}) = \lambda \lim_{T \to \infty} d_1\big(f(\mathbf{Y}), f(\hat{\mathbf{Y}})\big) \quad \text{a.s.,} \tag{35}$$

and furthermore rewrite (33) as

$$\bar{D} = \lambda \lim_{T \to \infty} \mathsf{E}\big[d_1\big(f(\mathbf{Y}), f(\hat{\mathbf{Y}})\big)\big] = \lambda D \quad \text{a.s.} \tag{36}$$

[4]Note that the rate-distortion function in Theorem 7 is in *bits per symbol*, while the rate-distortion function in Theorem 12 is in *bits per unit time*.

Similarly, we have

$$R_{\text{Poisson}}(\bar{D}) = \lambda R_{\text{Exponential}}(\bar{D}/\lambda) \tag{37}$$

and (34) follows by applying (21) of Theorem 7. ∎

Note that we have derived a lower bound for the Poisson-ℓ_1 rate-distortion function (Theorem 12) as a consequence of the exponential-ℓ_1 rate-distortion problem (Theorem 7). We observe that the resulting lower bound in (34) turns out to be the rate-distortion function as when the distortion measure is the canonical queuing [8] or the point covering distortion [9], [10]. This is not a mere coincidence, and we will come back to this in a later publication where we will discuss as to why these different distortion measures yield the same rate-distortion functions.

APPENDIX A
PROOF OF PROPOSITION 2

The proof is based on a "successive slicing" argument that shows that the $(n-1)$-dimensional volume of the intersection of the small ℓ_1^n-ball with the large sphere is not larger than the total surface volume of the small ball.

Let $\mathbb{K}$ be the smallest set containing open half-spaces $\mathcal{K}_i$ such that

$$\bigcap_i (\mathbb{R}^n \setminus \mathcal{K}_i) = \mathcal{B}_1^n(r_{\mathsf{b}}). \tag{38}$$

Note that the size of $\mathbb{K}$ is finite, namely 2^n (because $\mathcal{B}_1^n(r_{\mathsf{b}})$ has 2^n facets).

For $\mathcal{B}_1^n(r_{\mathsf{s}}, \mathbf{z}) \cap \mathcal{S}_1^{n-1}(r_{\mathsf{b}}) = \emptyset$, the claim trivially holds. Therefore we pick some $\mathbf{z}$ such that $\mathcal{B}_1^n(r_{\mathsf{s}}, \mathbf{z}) \cap \mathcal{S}_1^{n-1}(r_{\mathsf{b}}) \neq \emptyset$. Let $\mathcal{M} \triangleq \mathcal{B}_1^n(r_{\mathsf{s}}, \mathbf{z})$ be the small ℓ_1^n-ball, and define

$$\mathbb{L} \triangleq \{\mathcal{K} \in \mathbb{K} : \mathcal{K} \cap \mathcal{M} \neq \emptyset\} \subseteq \mathbb{K}. \tag{39}$$

We now go through the following algorithm:

1) While $\mathbb{L} \neq \emptyset$:
   a) Choose any $\mathcal{L} \in \mathbb{L}$.
   b) Slice off that part of $\mathcal{M}$ that intersects with $\mathcal{L}$:

$$\mathcal{M} \leftarrow \mathcal{M} \setminus (\mathcal{M} \cap \mathcal{L}). \tag{40}$$

   c) Remove $\mathcal{L}$ from $\mathbb{L}$:

$$\mathbb{L} \leftarrow \mathbb{L} \setminus \mathcal{L}. \tag{41}$$

2) Return $\mathcal{M}$.

Firstly, note that the algorithm will terminate in a finite number of steps because $\mathbb{L}$ contains a finite number of elements. Secondly, observe that in each iteration, the boundary measure of $\mathcal{M}$ is reduced. Thus, the boundary measure of the initial $\mathcal{M}$ is greater or equal to the boundary (denoted ∂) measure of the returned $\mathcal{M}$:

$$\text{vol}_{n-1}\left(\mathcal{S}_1^{n-1}(r_{\mathsf{s}}, \mathbf{z})\right) \geq \text{vol}_{n-1}\left(\partial\left(\mathcal{B}_1^n(r_{\mathsf{s}}, \mathbf{z}) \cap \mathcal{B}_1^n(r_{\mathsf{b}})\right)\right). \tag{42}$$

And since we also have

$$\text{vol}_{n-1}\left(\partial\left(\mathcal{B}_1^n(r_{\mathsf{s}}, \mathbf{z}) \cap \mathcal{B}_1^n(r_{\mathsf{b}})\right)\right)$$
$$\geq \text{vol}_{n-1}\left(\mathcal{B}_1^n(r_{\mathsf{s}}, \mathbf{z}) \cap \mathcal{S}_1^{n-1}(r_{\mathsf{b}})\right), \tag{43}$$

the claim follows.

APPENDIX B
PROOF OF PROPOSITION 9

For a regular simplex, the maximal hyperplane section is its facet [11, Sec. 5]. In this proposition, $\mathcal{U}_1^n(1)$ (an irregular n-simplex) is the convex hull (denoted $\text{co}(\cdot)$) of a regular $(n-1)$-simplex with $\mathbf{0}$, i.e., $\mathcal{U}_1^n(1) = \text{co}\left(\triangle^{n-1}(1), \mathbf{0}\right)$. Denote the origin of $\mathbb{R}^n$ by O, and let $P \in \mathbb{R}^n$ be the orthogonal projection of O onto $\triangle^{n-1}(1)$. Then we define $O' \in \mathbb{R}^n$ such that

$$\overrightarrow{PO'} = \sqrt{n+1} \cdot \overrightarrow{PO}, \tag{44}$$

and note that $\text{co}\left(\triangle^{n-1}(1), O'\right)$ is a regular n-simplex. We denote this regular n-simplex by $\triangle_{\text{reg}}^n$. Clearly,

$$\mathcal{U}_1^n(1) = \text{co}\left(\triangle^{n-1}(1), O\right) \tag{45}$$
$$\subset \text{co}\left(\triangle^{n-1}(1), O'\right) \tag{46}$$
$$= \triangle_{\text{reg}}^n. \tag{47}$$

Since the maximal hyperplane section of $\triangle_{\text{reg}}^n$ is its facet, $\triangle^{n-1}(1)$ is a maximal section of $\triangle_{\text{reg}}^n$. And because $\mathcal{U}_1^n(1)$ is a subset of $\triangle_{\text{reg}}^n$ (see (46)), $\triangle^{n-1}(1)$ is also a maximal section of $\mathcal{U}_1^n(1)$, i.e., for any hyperplane $\mathcal{K} \in \mathbb{R}^n$,

$$\text{vol}_{n-1}\left(\triangle^{n-1}(1)\right) = \max_{\mathcal{K}} \text{vol}_{n-1}\left(\mathcal{K} \cap \mathcal{U}_1^n(1)\right). \tag{48}$$

REFERENCES

[1] S. M. Moser, *Advanced Topics in Information Theory (Lecture Notes)*, 4th ed. Signal and Inf. Proc. Lab., ETH Zürich, Switzerland, and Inst. Commun. Eng., Nat. Chiao Tung Univ., Hsinchu, Taiwan, 2019. [Online]. Available: https://moser-isi.ethz.ch/scripts.html

[2] T. M. Cover and J. A. Thomas, *Elements of Information Theory*, 2nd ed. New York, NY, USA: Wiley, 2006.

[3] S. M. Moser, *Information Theory (Lecture Notes)*, 6th ed. Signal and Inf. Proc. Lab., ETH Zürich, Switzerland, and Inst. Commun. Eng., Nat. Chiao Tung Univ., Hsinchu, Taiwan, 2018. [Online]. Available: https://moser-isi.ethz.ch/scripts.html

[4] D. J. Sakrison, "A geometric treatment of the source encoding of a Gaussian random variable," *IEEE Trans. Inf. Theory*, vol. 14, no. 3, pp. 481–486, May 1968.

[5] T. R. Fischer, "A pyramid vector quantizer," *IEEE Trans. Inf. Theory*, vol. 32, no. 4, pp. 568–583, Jul. 1986.

[6] S. Verdú, "The exponential distribution in information theory," *Problemy Peredači Informacii (Problems of Inf. Transm.)*, vol. 32, no. 1, pp. 100–111, Jan.–Mar. 1996.

[7] H. Si, O. O. Koyluoglu, and S. Vishwanath, "Lossy compression of exponential and Laplacian sources using expansion coding," in *Proc. IEEE Int. Symp. Inf. Theory*, Honolulu, HI, USA, Jun. 29 – Jul. 4, 2014, pp. 3052–3056.

[8] T. P. Coleman, N. Kiyavash, and V. G. Subramanian, "The rate-distortion function of a Poisson process with a queueing distortion measure," in *Proc. Data Compression Conf.*, Snowbird, UT, USA, Mar. 25–27, 2008, pp. 63–72.

[9] A. Lapidoth, A. Malär, and L. Wang, "Covering point patterns," in *Proc. IEEE Int. Symp. Inf. Theory*, St. Petersburg, Russia, Jul. 31 – Aug. 5, 2011, pp. 51–55.

[10] ——, "Covering point patterns," *IEEE Trans. Inf. Theory*, vol. 61, no. 9, pp. 4521–4533, Sept. 2011.

[11] H. Dirksen, "Sections of the regular simplex – volume formulas and estimates," *Math. Nachr.*, vol. 290, no. 16, pp. 2567–2584, Nov. 2017.